

# XMM-Newton CCF Release Note

XMM-CCF-REL-177

## Low energy noise rejection refinement for pn.

M. Kirsch

September 15, 2004

### 1 CCF components

Name of CCF	VALDATE	List of Blocks changed	CAL VERSION	XSCS flag
EPN_REJECT_0002	2000-01-01T00:00:00	CORRECTION_VALUES	3.152	NO

### 2 Changes

The CCF contains the information how incorrect offset shifts for specific pixels can be reconstructed from the brightness of these pixels at 20 adu. This information was derived from correlating the 20 adu brightness with the corresponding value in the residual offset map. As the 20 adu brightness is also influenced by other effects, an image containing the median of several 20 adu images was subtracted before computing the correlation. This was the method used for deriving the values in `EPN_REJECT_0001.CCF`.

In the meantime it turned out that also the values in the residual offset maps are influenced by other effects, similar to the situation with the 20 adu images. Subtracting the median of several residual offset maps (which contain the temporally stable features) before correlating them with the residual 20 adu images reduced the scatter and led to an improved correlation. This was the motivation for the update of the CCF:

`EPN_REJECT_0001.CCF`:

derived from correlation of (20 adu brightness - median 20 adu brightness) with residual offset

`EPN_REJECT_0002.CCF`:

derived from correlation of (20 adu brightness - median 20 adu brightness) with (residual offset - median residual offset)

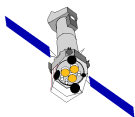


Figure 1 shows the original correlation, used for deriving the values in EPN\_REJECT\_0001.CCF

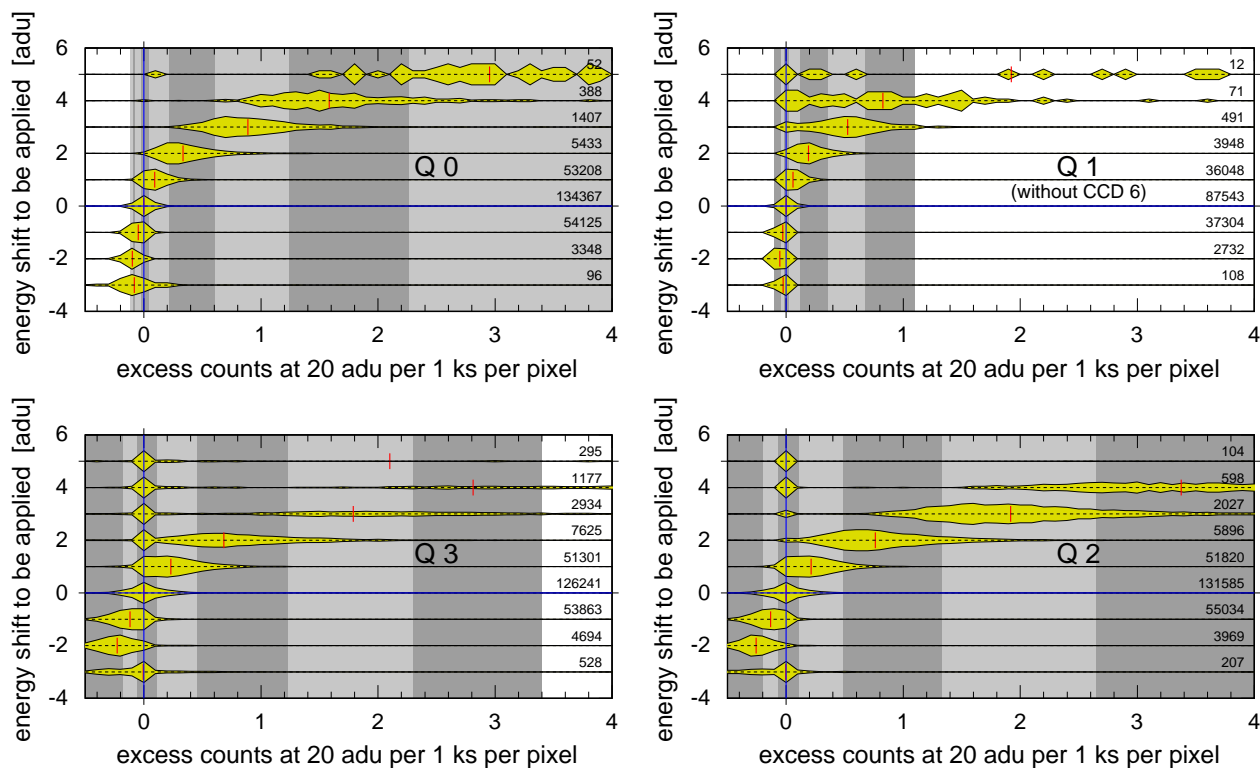


Figure 1: Pixel by pixel correlation between the excess counts at 20 adu, normalized to 1 ks, and the values in the (**uncleaned**) offset map, for all quadrants (arranged according to their position on the detector). While the energy shifts to be applied can only occur as integer multiples of 1 adu ( $\sim 5$  eV), the excess counts exhibit a much smoother distribution due to their normalization to 1 ks. Their distribution is illustrated by the thickness of “histogram tubes”, which were all expanded to have the same maximum thickness. The number of pixels which they contain are given at right. This correlation was derived by combining the observations of the Lockman hole in XMM revolutions 522, 523, 525, 526, 527, 528, and 544 ( $\sim 636$  ks total exposure time), all taken in fullframe mode. **For Q 1, exclusion of CCD 6 was necessary in order to get a better correlation.** For Q 3, four noisy columns were excluded. A vertical red line indicates the median value of the distributions. Shaded areas show the ranges of excess counts for which a certain energy shift should be applied. Note how the brightness of pixels at 20 adu responds differently in the four quadrants to energy shifts. No such variation was found within the CCDs of the same quadrant. K. Dennerl (MPE)

Figure 2 shows the improved correlation, used for deriving the values in EPN\_REJECT\_0002.CCF.

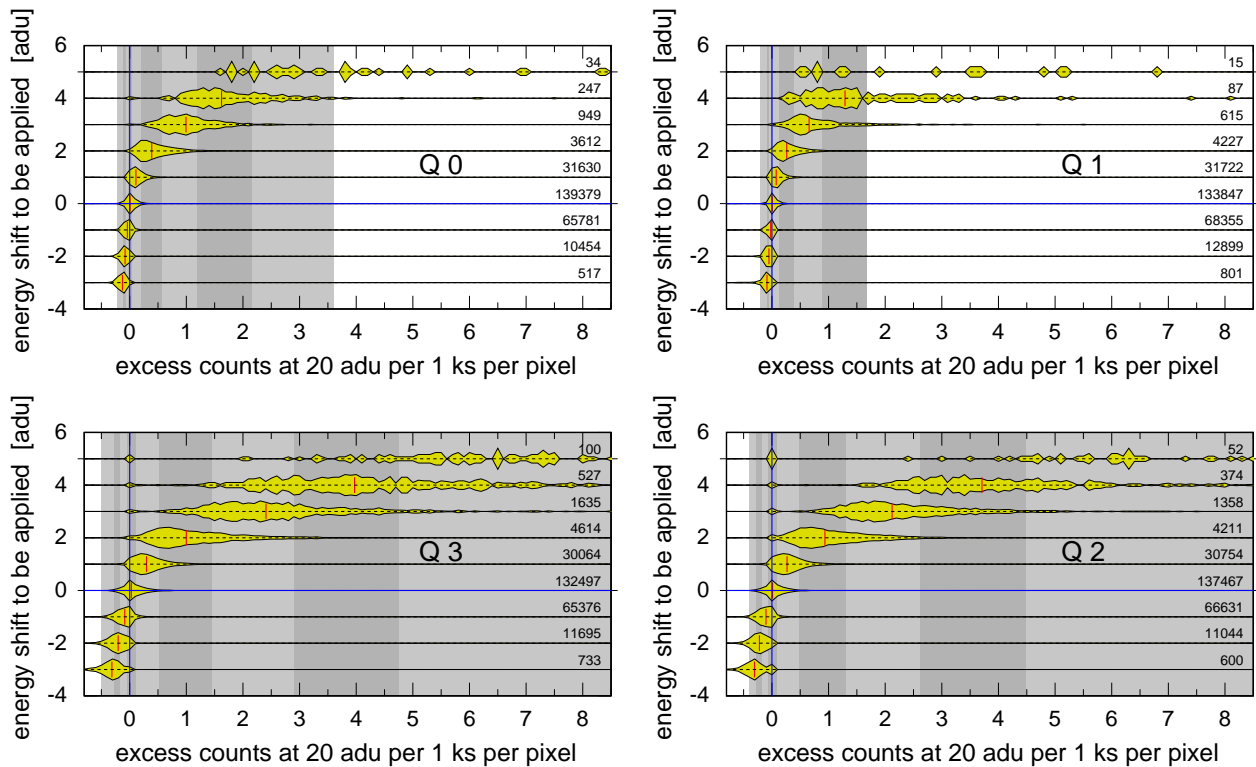
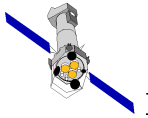
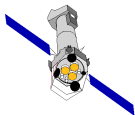


Figure 2: Pixel by pixel correlation between the excess counts at 20 adu, normalized to 1 ks, and the values in the **cleaned** offset map, for all quadrants (arranged according to their position on the detector). While the energy shifts to be applied can only occur as integer multiples of 1 adu ( $\sim 5$  eV), the excess counts exhibit a much smoother distribution due to their normalization to 1 ks. Their distribution is illustrated by the thickness of “histogram tubes”, which were all expanded to have the same maximum thickness. The number of pixels which they contain are given at right. This correlation was derived by combining the observations of the Lockman hole in XMM revolutions 522, 523, 525, 526, 527, 528, and 544 ( $\sim 636$  ks total exposure time), all taken in fullframe mode. For Q3, four noisy columns were excluded. **No exclusion of CCD 6 was necessary.** A vertical red line indicates the median value of the distributions. Shaded areas show the ranges of excess counts for which a certain energy shift should be applied. Note how the brightness of pixels at 20 adu responds differently in the four quadrants to energy shifts. No such variation was found within the CCDs of the same quadrant. From Dennerl et al., Proc. SPIE 2004 (Glasgow)

More information can be found in Dennerl et al., Proc. SPIE 2004, which describes specifically how EPN\_REJECT\_0002.CCF was obtained.

### 3 Scientific Impact of this Update

The differences to the results obtained with EPN\_REJECT\_0001.CCF are very subtle, however treat the behavior of the variation of the residual offset maps in the correct way.



## 4 Estimated Scientific Quality

The offset correction recovers errors of up to several 10 eV for point sources that happen to fall on a bright patch caused by a wrong offset value.

The reduction of the detector noise allows to extend the useful energy range down to an instrumental energy of 120 eV. Note that Figure 3 is not showing the difference between images processed with `EPN_REJECT_0001.CCF` and `EPN_REJECT_0002.CCF`, but the differences between the original image and the image after correcting the offset shifts with `EPN_REJECT_0002.CCF`. A comparison of `EPN_REJECT_0001.CCF` and `EPN_REJECT_0002.CCF` in images will not show any obvious differences.

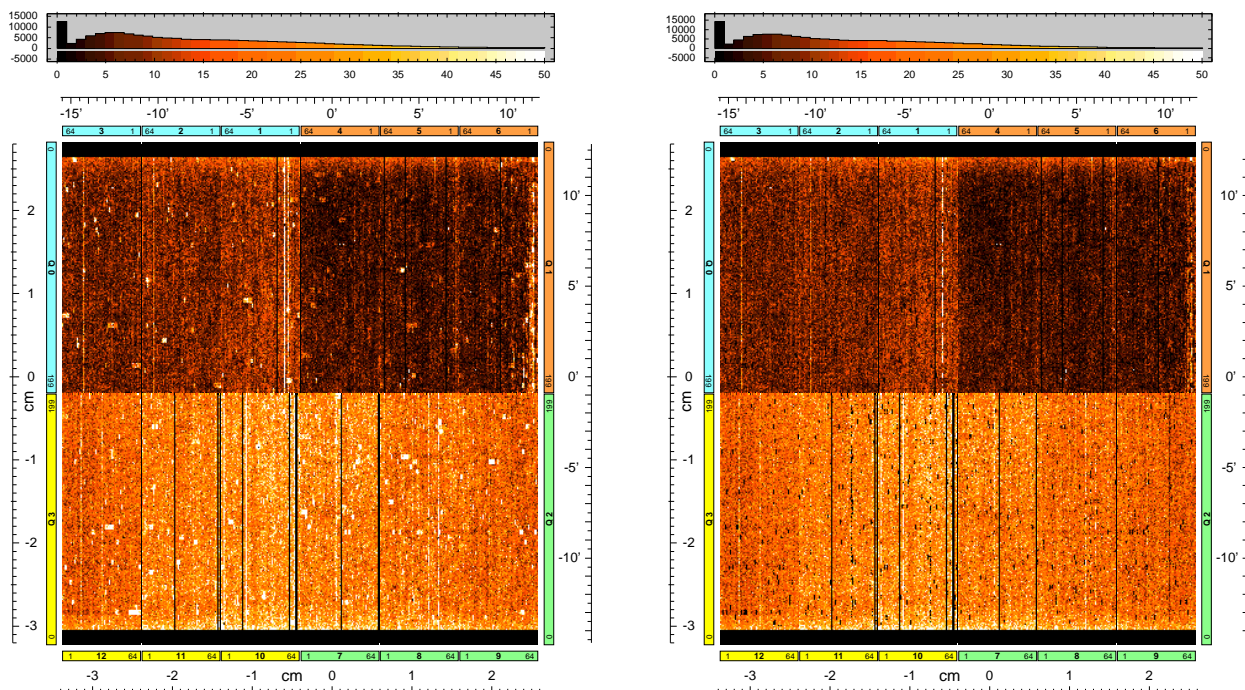
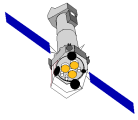


Figure 3: Images of all events with 20 adu in the data set 0367\_0137550901. Left: original image, right: image after correcting the offset shifts with `EPN_REJECT_0002.CCF`. Black pixels are caused by the fact that the offsets applied on-board were higher than 20 adu, so that there are no 20 adu data available. This problem disappears above  $\sim 22$  adu.

## 5 Test procedures & results

Tests were performed with the data set 0367\_0137550901, a 30 ks observation of the Vela SNR in FF mode. In general, the differences to the results obtained with `EPN_REJECT_0001.CCF` are very subtle.



## 6 Expected Updates

The first part of this task (the energy shift correction) is particularly important for observations where the offset map was not transmitted. For more recent observations, where the corresponding offset map is available, the offset shifts can be directly derived from the offset map. That is not yet implemented.